From microplastics to pixels: Testing the robustness of two machine learning approaches for automated, Nile red-based marine microplastic identification

Authors

Nelle Meyers[1,2,3,*], Bavo De Witte[2], Natascha Schmidt[4,5], Dorte Herzke[4,6], Jean-Luc Fuda[5], David Vanavermaete[2], Colin R. Janssen[3,7], Gert Everaert[1]

*Corresponding author. E-mail address: nelle.meyers@vliz.be

Affiliations

[1]Flanders Marine Institute (VLIZ), InnovOcean Campus, Jacobsenstraat 1, 8400 Ostend, Belgium.

[2]Flanders Research Institute for Agriculture, Fisheries and Food (ILVO), Animal Sciences Unit - Aquatic Environment and Quality, InnovOcean Campus, Jacobsenstraat 1, 8400 Ostend, Belgium.

[3]Department of Animal Sciences and Aquatic Ecology, Blue Growth Research Lab, Ghent University, 9000 Gent, Belgium.

[4]NILU, The FRAM Centre, P.O. Box 6606, 9296 Tromsø, Norway.

[5]Aix Marseille University, Toulon University, CNRS, IRD, Mediterranean Institute of Oceanography (MIO) UM 110, Marseille, France.

[6]Norwegian Institute for Public Health (NIPH), P.O.Box 222 Skøyen, 0213 Oslo, Norway.

[7]Blue Growth Research Lab, Ghent University, Bluebridge, Wetenschapspark 1, 8400 Ostend, Belgium.

Keywords

Microplastics; Machine learning; Automation; Fluorescence; Nile red; Weathered plastics; Monitoring; Marine pollution

Abstract

Despite the urgent need for accurate and robust observations of microplastics in the marine environment to assess current and future environmental risks, existing procedures remain labour-intensive, especially for smaller-sized microplastics. In addition to this, microplastic analysis faces challenges due to environmental weathering, impacting the reliability of research relying on pristine plastics. This study addresses these knowledge gaps by testing the robustness of two automated analysis techniques which

combine machine learning algorithms with fluorescent colouration of Nile red (NR)-stained particles. Heterogeneously shaped uncoloured MPs of various polymers—polyethylene (PE), polyethylene terephthalate (PET), polypropylene (PP), polystyrene (PS), and polyvinyl chloride (PVC)—ranging from 100 to 1000 µm in size and weathered under semi-controlled surface and deep-sea conditions, were stained with NR and imaged using fluorescence stereomicroscopy. This study assessed and compared the accuracy of decision tree (DT) and random forest (RF) models in detecting and identifying these weathered plastics. Additionally, their analysis time and model complexity were evaluated, as well as the lower size limit (2 – 4 µm) and the interoperability of the approach. Decision tree and RF models were comparably accurate in detecting and identifying pristine plastic polymers (both > 90%). For the detection of weathered microplastics, both yielded sufficiently high accuracies (> 77%), although only RF models were reliable for polymer identification (> 70%), except for PET particles. The RF models showed an accuracy > 90% for particle predictions based on 12-30 pixels, which translated to microplastics sized < 10 µm. Although the RF classifier did not produce consistent results across different labs, the inherent flexibility of the method allows for its swift adaptation and optimisation, ensuring the possibility to fine-tune the method to specific research goals through customised datasets, thereby strengthening its robustness. The developed method is particularly relevant due to its ability to accurately analyse MPs weathered under various marine conditions, as well as ecotoxicologically relevant MP sizes, making it highly applicable to real-world environmental samples.

1. Introduction

Microplastics (MPs), plastic particles ranging from 1 µm to 5 mm (Hartmann et al., 2019; Arthur et al., 2009), are a widespread and persistent pollutant, detected even in remote areas far from human activities (Peeken et al., 2018; Bergmann et al., 2019; Ross et al. 2021, Van Cauwenberghe et al., 2013, Peng et al., 2018). Accurate and robust observations are essential for evaluating the current and future environmental risks posed by MPs, however, MP analysis continues to be labour-intensive to this day (Primpke et al., 2020a). Indeed, analytical identification of MPs in a wide range of marine environmental matrices is a critical yet challenging part of the research. Consequently, an extensive spectrum of analytical methods has been developed in the last decade to meet a variety of research and monitoring purposes, based on the requirements associated with research and monitoring observations of MPs. However, many of these

techniques have considerable limitations in terms of resolution, minimum particle size, human bias interference, labour intensity and analysis time, and consequently, analysis cost (Primpke et al., 2020a).

Fluorescence microscopy, combined with fluorescent dyes, allows to effectively visualise MPs. The fluorescent dye Nile red (NR) has been widely used in MP studies because of its high adsorption for plastics, its affinity for a wide range of polymers, its short incubation time (10-30 min), and its effectiveness to detect MPs down to a few µm (Maes et al., 2017; Shruti et al., 2022). Nile red fluorescence of MPs is often imaged using fluorescence microscopes equipped with a camera, for subsequent visual or automated image analysis. A major flaw of the NR approach is the co-staining of lipid-rich organic material, which interferes with MP analysis (e.g. Maxwell et al., 2020; Shruti et al., 2022). However, false positives resulting from this issue can be mitigated using a multiple-filter approach (Meyers et al., 2022).

The integration of automation into various MP detection and identification techniques has recently led to a remarkable transformation in MP research. The application of Artificial Intelligence (AI) in the field of research has revolutionised the way researchers approach MP analysis, with machine learning (ML) gaining particular popularity as it enables a faster, more cost-effective, and less biased particle identification (Guo et al., 2024). Numerous prediction models based on ML have been developed for the automated detection and identification of MPs, where the main principles often rely on vibrational spectroscopy (Lin et al., 2022). Frequently used algorithms to do so include decision trees (DTs), random forests (RFs), support vector machines, K-nearest neighbours, and neural networks (Yan et al., 2022; Lin et al., 2022). Automation of MP analysis methods has however introduced both opportunities and challenges. Selecting the best model is data-dependent, where finding a trade-off between model performance, model complexity and computational speed is crucial (Maxwell et al., 2018). Machine learning programs can process large amounts of data with a high accuracy but can take up a lot of time to do so, especially when limited computing power is available, making it costly. For example, Focal Plane Array (FPA) array-based µ-FTIR images combined with a spectroscopic analysis pipeline allows for the automated comparison of MP polymers and their unique infrared spectra with spectral libraries using pattern recognition algorithms, but overall analysis time is still relatively high (Primpke et al., 2017). For instance, it may take 4 h to scan 14 x 14 mm with a pixel resolution around 11 µm (64 x 64 FPA detector elements) (Bergmann et al., 2019; Primpke et al., 2020a), while an additional 4 – 48 h is needed for spectral analysis by spectral correlation (Peeken et al., 2018; Primpke et al., 2020b; Primpke et al., 2020a). A compromise between model complexity and model performance also exists: although they often perform

96 better, more complex ML algorithms such as RFs lack transparency as they are much harder to interpret,
97 especially for non-experts in the field of AI (Breiman et al., 1993; Breiman et al., 2001; Witten et al., 2002).
98 Simpler models like DTs are more intuitive and easier to interpret due to their transparency. However,
99 they are less effective for complex or noisy datasets and are more prone to overfitting, which occurs when
100 a ML model performs significantly better on training data than it does on new datasets (Breiman et al.,
101 1993; Breiman et al., 1996; Witten et al., 2002).
102
103 Microplastics in the marine environment undergo weathering, e.g. due to mechanical forces, UV radiation,
104 microbial colonisation, and hydrostatic pressure, leading to alterations in their physical and chemical
105 structure (Fotopoulou et al., 2019; Shah et al., 2008; Fauvelle et al., 2021). These changes can complicate
106 their detection and analysis (Dong et al., 2020; Liu et al., 2020), underscoring the need to consider
107 weathered MPs in method development, effect studies, and leaching experiments, along with their
108 pristine representatives. Standard Raman and IR spectra of MPs were shown to be significantly impacted
109 by environmental weathering processes through shifts in their spectra (Dong et al., 2020) which in turn
110 can interfere with the spectral matching process. Shifts in crystallinity and polarity (Maes et al., 2017) can
111 also impact the fluorescence of NR-stained plastics due to the solvatochromism of the dye, i.e. its
112 fluorescence changes based on the polarity of its environment, in this way affecting the accuracy of the
113 approach.
114
115 At present, the bulk of method development-focused research and effect studies still relies on pristine
116 MPs (Waldman and Rillig, 2020; Alimi et al., 2022), yet recent studies suggest that aged plastics behave
117 differently (Arp et al., 2021; Bhagat et al., 2022). This underlines the importance of implementing
118 environmentally relevant MPs into future MP research for more accurate findings. To tackle this problem,
119 MP structural and chemical transformations brought on by weathering processes are nowadays being
120 studied during laboratory simulations. However, most research focuses only on a few ageing processes
121 when mimicking environmentally relevant conditions (Alimi et al., 2022), while the degradation of MPs in
122 the marine environment is influenced by fluctuations in weathering processes and abiotic factors like
123 seawater temperature, salinity and hydrostatic pressure. In addition, degradation is affected by the
124 polymer type, size, structure, shape, and density of MPs. The complex interplay between these variables
125 makes it difficult to realistically simulate MP degradation in a laboratory setting.
126

There is still much to uncover regarding the abundance, behaviour, and potential effects of smaller-sized MPs (< 100 µm). While methods capable of reaching this MP size threshold exist, the time and costs involved in analysis hinder routine assessments, emphasising the need for cost-efficient and high-throughput analysis methods. Moreover, smaller-sized MPs are an emerging concern in the field of ecotoxicology (Beiras et al., 2020). A smaller size translates into an increased surface-to-volume ratio of MPs, which renders them more bioavailable (Mattsson et al., 2015, Wagner and Reemtsma, 2019). Their size can also accelerate physicochemical and biochemical reactions at their surface (Wayman et al., 2021). This disparity between current analysis methodologies and ecotoxicologically relevant MP sizes stresses the existing gap in our understanding of the true extent and impact of MP contamination in the marine environment. Addressing this issue is therefore imperative for a comprehensive assessment of MP pollution.

A last significant challenge MP research faces is the interoperability of analysis methods. Ensuring a constant performance of a method across different laboratories, regardless of the diverse laboratory conditions, is of paramount importance in scientific research. Consistency across various laboratories strengthens the credibility of obtained findings using that method, creates a sense of confidence in the scientific community, and hence encourages the widespread adoption and application of a method. This in turn contributes to a more comprehensive understanding and management of MP pollution in marine ecosystems.

Despite the urgent need for accurate and robust observations of MPs to assess environmental risks, many existing methods are labour-intensive and costly and may not always guarantee consistent performance across different laboratories. Moreover, current research often relies on pristine plastics, overlooking the complexities introduced by environmental weathering, which can alter the physical and chemical properties of MPs and impact analytical reliability. Additionally, there is a significant gap in cost-efficient methods for analysing smaller, ecotoxicologically relevant MPs. In response to the current shortcomings, this research focused on testing the robustness of two recently developed, automated, Nile-red (NR) based MP analysis techniques, created using two different ML algorithms. To do so, their ability to accurately analyse MPs weathered under semi-controlled surface water and deep-sea water conditions was assessed and compared, along with their analysis time and model complexity. Additionally, the size limit of the overall best performing technique was determined, i.e. the minimum particle size for which the model algorithm produces sufficiently accurate predictions in terms of plastic identity and polymer

type. Finally, we tested whether the knowledge rules generated by this classifier produce consistent results across different labs. The novelty of the developed method lies in its broad applicability, as it covers a diverse range of plastic polymers, weathering conditions, and instrumentation types, providing a comprehensive tool for advancing MP research. By verifying the robustness of the models, we assess their reliability for widespread adoption and application, which serves as a cornerstone for a comprehensive understanding and effective management of MP pollution within a marine context.

2. Materials and Methods

This work used an open-source approach that combines NR-stained particle fluorescence with machine learning models, following a comprehensive six-step protocol. First, two sets of Red, Green, and Blue (RGB) colour datasets were created using two types of microscopes: a fluorescence stereomicroscope (FSM) and a fluorescence microscope (FM). Each set had two datasets for training a 'Plastic Detection Model' (PDM) to classify particles as plastic or non-plastic, and a 'Polymer Identification Model' (PIM) to classify plastic particles by polymer type (Fig. 1 - step 1). This was done as per Meyers et al 2022 and Meyers et al., 2024a, where RGB-colour values extracted from pixels of particles photographed with a fluorescence microscope were used to generate RGB statistics that make up the datasets, which in turn were used to train models and make predictions of a particle's identity based on its RGB statistics. The first set of RGB datasets, constructed at the laboratory of the Flanders Research Institute for Agriculture, Fisheries and Food (ILVO set with ILVO datasets 1 and 2) were used to generate and validate a total of five ILVO PDMs and five ILVO PIMs, and this using two types of ML algorithms, i.e. a decision tree (DT) and a random forest (RF) classifier (Fig. 1 - step 1). To do so, the datasets were split into 80% training data and 20% test data.

Secondly, the average number of correctly classified instances (CCI) + standard deviation (SD) (%) for a subset of particles unknown to the models (test datasets) was calculated for each of the models, and compared for both classifiers: plastic/non-plastics for the PDMs, and polymer type for the PIMs. Cohen's Kappa statistic, used to compare observed accuracies with expected accuracies, was also calculated (Fig. 1 - step 2). Running five simulations per model (PDM/PIM) for each classifier enhanced the robustness and reliability of the evaluation process by mitigating the influence of random variations or chance occurrences on model performance. Thirdly, after also comparing their analysis time and model complexity (cfr. '2.2 Model construction and classifier comparison') for the overall best scoring model

algorithm, the average accuracy of the ILVO models based on the best performing ML algorithm was tested for the detection and identification of MPs weathered at sea under semi-controlled, surface water and deep-sea water conditions for a duration of 12 months using five simulations per model type (Fig. 1 - step 3).

As a fourth step, a second set of models was constructed and validated, using the second set of RGB datasets constructed at the laboratory of the Flanders Marine Institute (VLIZ set with VLIZ datasets 1 and 2), which comprised RGB data from images acquired at a higher magnification (VLIZ PDM and VLIZ PIM) (Fig. 1 - step 4) To do so, the existing RGB datasets from Meyers et al., 2022 were expanded. In the fifth step, the lower size limit of the developed approach was determined (cfr. '2.3 Lower size limit') using the VLIZ models with the highest magnification (Fig. 1 - step 5). In a sixth and last step, the interoperability of the approach was tested by evaluating the average performance of the ILVO models for the VLIZ datasets 1 and 2, and the performance of the VLIZ models for the ILVO datasets 1 and 2, based on five simulations per model type (Fig. 1 - step 6).

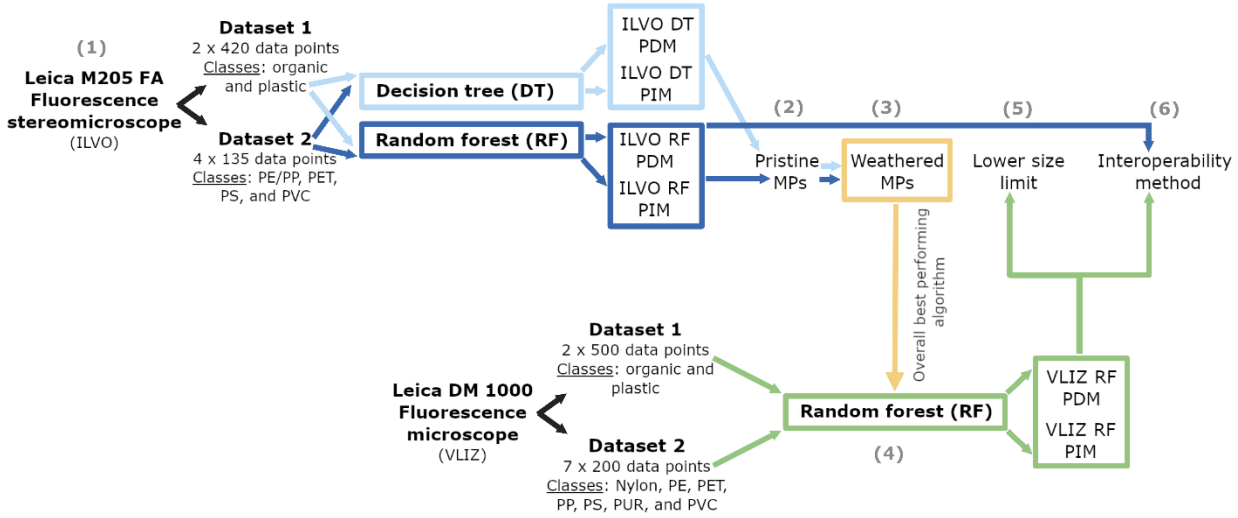

Fig. 1. Schematic overview. A schematic overview of the comprehensive, six-step approach employed in this work, where the robustness of a microplastic analysis method based on machine learning models combined with fluorescent colouration of NR-stained particles was thoroughly tested.

2.1 Construction of datasets

ILVO datasets 1 and 2 were based on images series acquired with a fluorescence stereomicroscope (Leica M205 FA Fluorescence stereomicroscope - LAS X software), at a magnification of 1 x 10, while images

series for the two VLIZ datasets were acquired with a fluorescence microscope (LEICA DM 1000 - Leica Application Suite version 4.13.0), at a 10 x 10 magnification (Fig. 1) (Meyers et al., 2024b). To generate the RGB datasets for the ILVO PIM and the VLIZ PIM (as described in detail in Meyers et al., 2022), five and seven of the most abundantly produced MP polymers globally, respectively, as well as organic materials with high prevalence in the marine environment were selected. First, uncoloured and pristine polyethylene (PE), polyethylene terephthalate (PET), polypropylene (PP), polystyrene (PS), and polyvinyl chloride (PVC) were obtained and cryomilled into heterogeneously shaped particles (50 - 1,200 µm) by specialized companies (Centexbel - Zwijnaarde, Belgium, and CARAT GmbH - Bocholt, Germany). The organic materials cotton, flax (raw and bleached), hemp (raw and bleached), silk, and wool (alpaca and sheep) were also obtained from Centexbel, while chitin, wood, and gull feathers were collected from the beach and cut into similarly sized particles. In the next step, less than 0.5 mg of each material (the different plastic polymers/organic material in general) was added to separate glass beakers containing Milli-Q water. To test the ability of the models to correctly classify unknown polymers as plastics, for the VLIZ PIM, two additional polymers were used, i.e. nylon and PUR particles. As PE and PP are similar with respect to their fluorescence as a consequence of their similar chemical structure (Meyers et al., 2022), it was decided to group them into one class to construct the ILVO PIM ('PE/PP'). All MPs used were pristine, heterogeneously shaped uncoloured fragments, with varying densities (Gago et al, 2019). Next, the content of each beaker was filtered over a PTFE-filter (47 mm diameter, 10 µm pore size, Millipore Ltd.) using a MilliPore manifold system (3 + 3 workstations) (Merck Millipore) and stained with 1 mL of the fluorescent dye Nile red dissolved in acetone (10 µg mL^{-1}) using a glass pipette. After 15 min, filters were rinsed with Milli-Q water and left to dry in a dark environment for 24 h.

Particles were photographed with both types of microscopes using fixed settings, capturing a series of 3 images per particle under a blue, green, and UV microscope filter (cfr. Table S1 for details). Red, Green, and Blue colour data from 135 (ILVO PIM) and 200 (VLIZ PIM) particles per plastic polymer type, or per group of plastics (PE/PP), were analysed to construct ILVO dataset 2 and VLIZ dataset 2 (n = 540 and n = 1400). A random subselection of MP particles, evenly spread across all polymers, was used to construct ILVO dataset 1 and VLIZ dataset 1, complemented with RGB data from 420 (ILVO PDM) and 500 (VLIZ PDM) particles of natural origin (n = 840 (2 x 420) and n = 1000 (2x 500)). For the VLIZ datasets, 15 - 50 images for each of the material types (i.e. all individual polymers, and a mix of organic materials) were used to build the datasets. Three PTFE filters per material type were used, acquired over three days. For the ILVO datasets, 6 images per material type, capturing an entire PTFE filter, were used. Six PTFE filters

per material were employed, acquired over three days. All dataset sizes allowed for an appropriate statistical power for a small effect size ($\alpha = 0.05$, power = 0.8) (Serdar et al., 2021). Required training dataset sizes of all four models for which prediction error was below 5% were also simulated using the randomForest package in R (Fig. S1) (Liaw & Wiener, 2002).

Once the images were acquired, extraction of the RGB values from particle pixels was done through automated image analysis in the open-source image processing program ImageJ (Abràmoff et al., 2004) according to the updated procedure described in Meyers et al., 2024a. For each particle above a set size limit within each image series, a CSV file was generated with extracted RGB values of all pixels lying on the maximum Feret diameter of that particle, and this for the image acquired under the blue, green and UV filter. Next, per particle, for each microscope filter, statistics were calculated (10th, 50th and 90th percentile as well as the mean value) for each of the three colour values (R, G, and B) in R (R Core Team, 2020). All 36 RGB statistics per particle were then automatically compiled into the above-mentioned datasets (cfr. Meyers et al., 2022 for method details).

2.2 Model construction and classifier comparison

For both classifiers (DT and RF), the generated RGB statistics were used as input variables, while the output was particle identity (plastic/non-plastic for the PDM and polymer type for the PIM). Decision tree classifiers create flowchart-like trees, where each internal node represents a test of a feature, the branches represent outcomes of the tests, and leaf nodes signify the output of the algorithm. The datasets were recursively split into smaller datasets based on the values of the features, i.e. the RGB statistics. The CART (Classification and Regression Tree) supervised ML algorithm (Therneau et al., 2015) was used to generate the DT classifiers (Meyers et al., 2022), (five simulations per model type) where, for the PDM and PIM, respectively, a minimum of 8 records had to be present in a node before a split was attempted, as well as a minimum of 3 records in an end node, and splits that did not enhance the model fit by 0.02 were eliminated. To avoid overfitting, the model was allowed to grow until a depth where the validation metrics used either stagnated or declined.

RF classifiers, on the other hand, average the output of multiple DTs fit on random subsamples (63.2%) of the dataset, and this to obtain a single result (bootstrap aggregating or bagging). Breiman's RF algorithm (Breiman, 2001; Liaw & Wiener, 2002) was used to construct the RF classifiers here, where a fitting number of variables (cfr. Fig. S2 "optimal number of parameters") were chosen each time at random out

of all predictor variables, and the best split on these variables was used to divide the node. For each tree, the leftover data (36.8%) was then used to calculate the misclassification rate, i.e. the out of bag (OOB) error rate. The aggregated error, which determines the overall OOB rate of the classifier, was plotted for each model as a validation. To fine-tune the RF models, the number of trees to achieve the most accurate results was also determined (Fig. S3). The final, optimised models all had 500 prediction trees (ntree), each using max. 12 variables (mtry).

To visualise classification performance of all four models, non-metric multidimensional scaling (NMDS) plots using the Bray-Curtis similarity index and default settings were generated in R (Fig. 2, Fig. S4) based on one of the five simulations for each model type. For both classifiers, the best features to split the data were based on the Gini impurity metric (Daniya et al., 2020). The accuracy of all models using both classifiers was assessed based on their CCI rate, their Cohen's kappa statistic (McHugh, 2012), which is a measure of interrater reliability, and their confusion matrices. For the DTs, this was done by randomly selecting 4/5 of each dataset to train each of the five models per model type and keeping the remaining 1/5 as a validation dataset based on the Pareto principle ratio (Dunford et al., 2014). For the RFs, five-fold cross-validations were performed to estimate the skill of the models on unseen data by re-training the models on the same design. Here, each dataset was split into five randomly chosen equal folds (each containing 1/5 of the dataset). Validation iterated over these folds, using each as a unique test dataset while training the model on the remaining four. Additionally, model training duration, analysis time, and complexity were assessed and compared for both classifier types. Furthermore, when the average overall model accuracy was < 70%, the model was considered unfit for MP analysis.

RGB datasets derived from pristine MPs were used to construct all models. While the conventional approach may be to train models on datasets developed using weathered plastics, logistical constraints underscore the challenge associated with this approach (discussed under '4.4 Interoperability'). While conducting an extensive weathering of various polymers under environmentally relevant conditions as done here is relevant and feasible (cfr. '2.3 Natural weathering of microplastics'), it implies that models could only be built once weathering is finalised. Therefore, the initial strategy focused on assessing the performance of RF models trained on pristine materials when applied to weathered MPs, providing a pragmatic foundation for subsequent investigations.

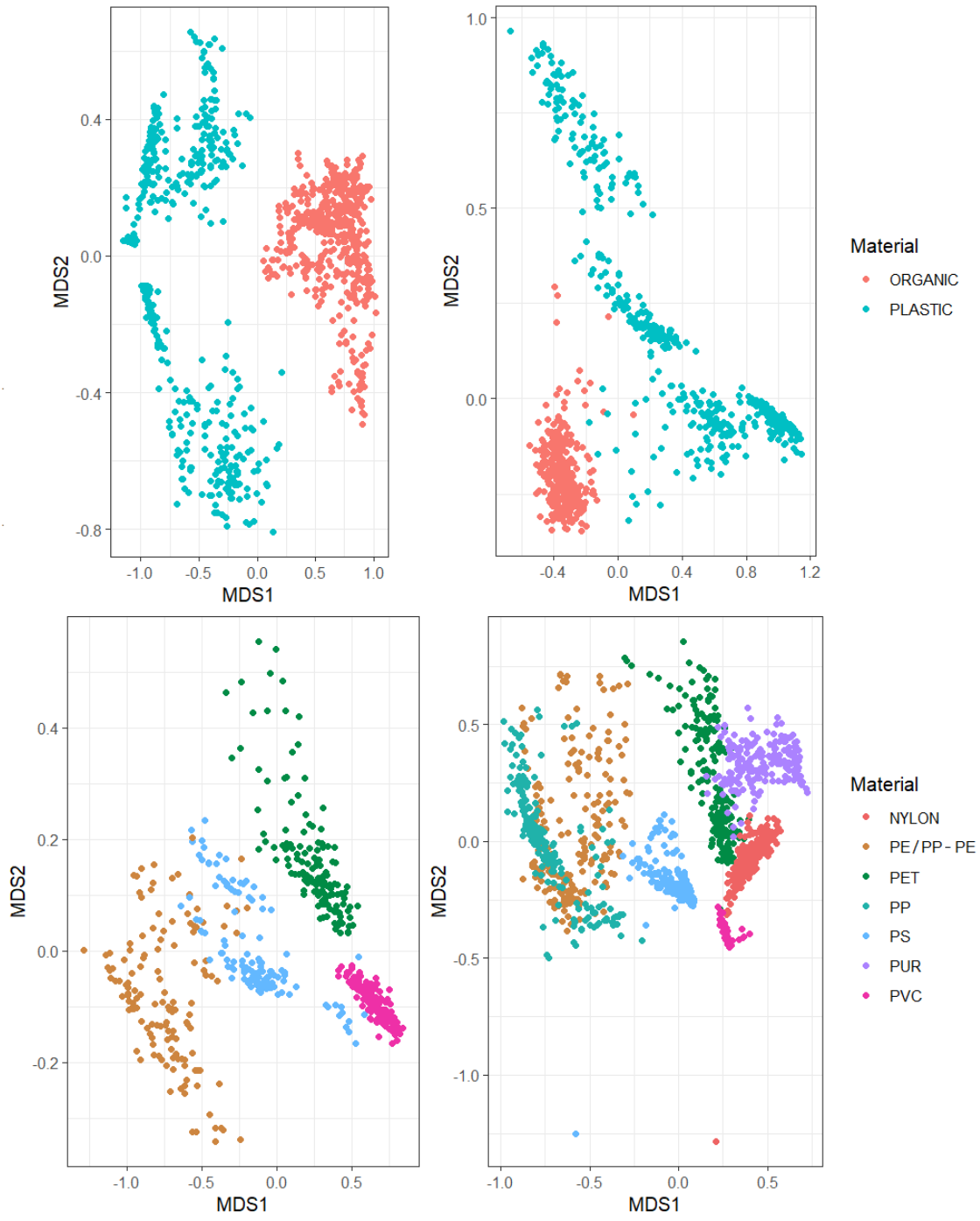

Fig. 2: Non-metric multidimensional scaling plots of the training datasets. The non-metric multidimensional scaling (NMDS) plots highlight the differences and similarities in fluorescent colouration of all Nile red-stained particles used to train the four models: from top to bottom, left to right: ILVO Plastic Detection Model (PDM), VLIZ PDM, ILVO Polymer Identification Model (PIM), VLIZ PIM.

2.3 Natural weathering of microplastics

To test the robustness of the classifiers, their ability to correctly classify naturally weathered plastics was tested. A mix of MP fragments (PE, PET, PP, PS, and PVC) sized 500 - 1000 µm (CARAT GmbH) was filled into stainless steel tubes (316 mesh) (Inoxia Ltd, 45.7 Dunsfold Park, Stovolds Hill, Cranleigh, GU6 8TB, United Kingdom), which were placed in stainless steel containers (Fig. 3). The containers were deployed in subsurface, coastal waters in the Norwegian Sea (Tromsø, Norway; 69.642730, 18.950389) in February 2021 and in deep-sea waters (2380 m depth) of the Mediterranean Sea (off the coast of Marseille, France; 42.807683, 6.043867) (Fig.3 and Fig. S5) in April 2021, respectively. During the exposure at sea, the stainless-steel containers deployed in subsurface waters were manually cleaned at regular intervals to remove bivalves and other attached organisms. The samples remained submerged in the sea for 12 months before being retrieved. Afterward, the stainless-steel tubes were left under a fume hood to dry. Next, the microplastic particles were transferred into burnt (450 °C, 6 h) glass vials and brought to the laboratory.

Following this, for each type of weathering, polymer particles were stained under the previously described conditions and photographed under the fluorescence stereomicroscope using the same settings as for pristine particles (Table S1). Hereafter, the average predictive performance of the FSM PDM and FSM PIM was tested using a random selection of 30 particles per polymer (PE/PP, PET, PS and PVC), for each type of weathering, totaling 240 particles. Additionally, ATR-FTIR spectra of each studied polymer were acquired in its pristine, surface water-weathered, and deep-sea water-weathered form (Perkin Elmer Frontier FTIR with UATR top plate with diamond/ZnSE crystal, Zaventem, Belgium). For clarity, deep-sea water-weathered (DSW) MPs and surface water-weathered (SFW) MPs will be referred to as DSW MPs and SFW MPs, respectively.

Fig. 3a, 3b and 3c. Controlled natural weathering of microplastics. Stainless steel tubes (3b) were filled with a microplastic mixture and placed inside stainless steel containers. These containers were then submerged in subsurface coastal waters of the Norwegian Sea near Tromsø, Norway (3a), or in the deep sea off the coast of Marseille, France, in the Mediterranean Sea, for a duration of 12 months. For the deep-sea deployment, the containers were mounted on a carousel (3c), which was retrieved after weathering using an acoustic release system (Fig. S5).

2.4 Lower size limit

To determine the lower size limit of the two best performing models, for PE, PS, PET and PVC, a small amount of MPs (<0.5 mg) sized < 5 µm - 300 µm was added to a glass beaker with Milli-Q water, whose content was then filtered and NR-stained (cfr. '2.1 Construction of datasets'). One filter per polymer was obtained and photographed using the fluorescence microscope, which offers the largest magnification of both microscope types (i.e. 10 x 10). Next, all MPs present were analysed using the VLIZ PDM and PIM, and the number of pixels per MP used to predict the particle identity was assessed. A total of 2010 PET particles, 3939 PE/PP particles, 1596 PS particles and 2533 PVC particles were analysed and subdivided into 10 different size groups (Table S2), representing all particles present on the PTFE filter per polymer. Following this, a graph was constructed to plot predictive accuracy per size class for the PDM and PIM. The lower size limit for each polymer type was determined as the smallest number of pixels and corresponding size class for which both models achieved an accuracy > 70 %.

362 2.5 Interoperability

363 To test the interoperability of the analysis method, MPs imaged with the Leica M205 FA Fluorescence
364 stereomicroscope were analysed using models trained on images from the LEICA DM 1000, and vice versa.
365 In this process, all particles of datasets 1 and 2 from the VLIZ laboratory were analysed using models
366 trained on datasets 1 and 2 from the ILVO laboratory, respectively, and vice versa.
367
368 2.6. QA/QC

369 As background control measures to prevent MP contamination, the use of plastic materials was avoided
370 prior to the image acquisition, tools and glassware used were pre-cleaned with Milli-Q water and soap
371 before use, sample processing was conducted in a laminar flow hood, and a 100% cotton lab coat and
372 trousers were worn. Additionally, a subset of pristine MPs to construct the models as well as the
373 weathered MPs were FTIR validated (cfr. Methods Supplement).
374

375 ## 3. Results

376

377 3.1 Classifier comparison for pristine materials

378 DT and RF classifiers both had high accuracies (> 90% for all models) based on the obtained CCI rates and
379 Cohen's kappa statistics (Table 1). Fluorescent colouration differed between plastic and organic particles,
380 as well as between most polymers, except for PP and PE (VLIZ PIM), as is apparent from the NMDS plots
381 (Fig. 2, Fig. 4, Fig. S4, Fig. S6). The PDMs based on both classifiers misclassified only a negligible number
382 of organic and plastic materials. The PIM built using the DT approach misidentified PS particles as PE (4.4
383 ± 9.9%), PET (2.2 ± 2%), and PVC (2.2 ± 3.3%). Additionally, it misclassified PE as PS (3 ± 3.1%), PET particles
384 as PVC (1.5 ± 2%), and PVC particles as PET (1.5 ± 2%) and PS (1.5 ± 2%). When using the RF approach,
385 classification errors primarily involved PE/PP particles being classified as PS (0.7 ± 0%), PET as PS (0.7 ±
386 0%), PS as PVC (1 ± 0.4%), and PVC as PS (0.7 ± 0%). For both classifiers, SDs were low and relatively
387 constant, indicating minimal variability among the five obtained accuracies for each of the models. Based
388 on model performances in Table 1, the accuracy of DT and RF classifiers was relatively similar for pristine
389 materials.
390
391
392

Table 1. Predictive accuracy of decision tree (DT) vs. random forest (RF) classifiers for pristine microplastics. Predictive accuracy of the Plastic Detection Model (PDM) and the Polymer Identification Model (PIM) for pristine MPs and organic material, based on DT and RF classifiers, using images acquired with a fluorescence stereomicroscope (FSM) (ILVO datasets 1 and 2).

	DECISION TREE CLASSIFIER		RANDOM FOREST CLASSIFIER	
PRISTINE PLASTICS FSM (ILVO)	PDM	PIM	PDM	PIM
CCI %	99.3 ± 1.1%	95.9 ± 2.3%	100 ± 0%	99 ± 0.5%
Cohen's κ	1	0.98	1	1
PE/PP		97 ± 3.1%		99.26 ± 0%
PET		98.5 ± 2%		99.26 ± 0%
PS		91.1 ± 8.1%		97.93 ± 1%
PVC		94 ± 1.7%		99.26 ± 0%
Organic material	99.8 ± 0.5%		100 ± 0%	

3.2 Classifier comparison for weathered MPs

When considering the average predictive reliability of the ILVO models for weathered MPs, model performance was very similar for DT and RF classifiers across different types of weathering (77.2 ± 38% vs. 78.8 ± 36% for SFW particles, and 86.8 ± 20.2% vs. 87.8 ± 17.1% for DSW particles, respectively) (Table 2). For SFW MPs, misclassifications were primarily PET particles classified as organic material (CCI rate of 20.7 ± 8.3% for DTs and 25.3 ± 1.8% for RFs). For DSW MPs, the main misclassifications involved PE/PP particles identified as organic material (CCI of 57.3% ± 8.3% and 63.3 ± 0%). Average accuracies were substantially higher for SFW particles when PET particles were excluded from the analysis, for both DT and RF classifiers (96 ± 6.9% vs. 96.7 ± 5.8%, respectively). In contrast, for DSW particles, excluding PET had a negligible effect on accuracy (85.8 ± 24.6% vs. 87.6 ± 21, respectively).

While the predictive accuracy of the PIM remained high for polymers such as PE/PP (SFW: 95.3 ± 3% and DSW: 98 ± 1.8%) and PS (only SFW: 89.3 ± 23.9%) using the DT classifier, PET and PVC showed substantial misclassification rates. For SFW and DSW MPs, respectively, PET had a CCI rate of 11.3 ± 7.7% and 36.7 ± 22.9%, while PVC had a CCI rate of 58.7 ± 14.3% and 57.3 ± 27.6%. Moreover, the predictive accuracies for PS showed a relatively large variability (SD of 23.9%), indicating inconsistent performance of the DT classifier for this polymer type.

When assessing the overall PIM performance, the RF classifiers outperformed the DTs. The average accuracies for RFs were 70 ± 39.2% for SFW MPs and 80.3 ± 14.8% for DSW MPs, compared to 63.7 ± 38.4% and 60.8 ± 26.3% for DTs, respectively. Similar to the PDM, the average accuracy for SFW particles substantially increased, and the SD decreased when PET particles were excluded (88.9 ± 12.8%). For DSW particles, the accuracy remained relatively consistent (84 ± 15.7%). For the DT classifiers, only the average predictive accuracy of the PDM exceeded the 70% threshold. In contrast, both the PDM and PIM exceeded this threshold when using the RF classifiers. The RF models were hence considered most reliable for the accurate identification of MP polymers, except for the analysis of SFW PET particles (accuracy of 25.3 ± 1.8%).

The fluorescent colouration and intensity of pristine and SFW PET particles differed considerably compared to other polymers, particularly under the blue filter, which is crucial for some model parameters (Fig. 4 and Fig. S7). Attenuated Total Reflectance (ATR) spectra of each polymer, acquired in their pristine, surface water-weathered, and deep-sea water-weathered forms, are freely available in the open-access repository Marine Data Archive (Meyers et al., 2024c), and are visualised in Fig. S8 - S12.

The ILVO PDMs and PIMs using DT classifiers consisted of five single trees, each based on different training datasets. The PDMs were pruned to a depth of 1, and had a total of 2 leaf nodes, while the PIMs were pruned to a depth of 5 to prevent overfitting, with a total of 9 leaf nodes, including multiple PE, PET, and PS and nodes. In contrast to these simpler models, the RF-based ILVO PDMs and PIMs required 100 trees each to produce accurate results, respectively (Fig. S3), with tree depths ranging from 1 - 5. Although model complexity increased, the computational time for generating predictions was < 10 s for both the DT and RF approaches.

Table 2A (upper) and 2B (lower): Predictive accuracy of decision tree (DT) (2A) vs. random forest (RF) (2B) classifiers for weathered microplastics. Predictive accuracy of the Plastic Detection Model (PDM) and the Polymer Identification Model (PIM) for surface water-weathered MPs and deep-sea water-weathered MPs using DT and RF classifiers.

	SURFACE WATER WEATHERED MPS		DEEP-SEA WATER WEATHERED MPS	
DECISION TREE CLASSIFIER FSM (ILVO)	PDM	PIM	PDM	PIM
CCI %	99.3 ± 1.1%	95.9 ± 2.3%	99.3 ± 1.1%	95.9 ± 2.3%
Cohen's κ	1	0.98	1	1
Total number of tested MPs	77.2 ± 38.1%	63.7 ± 38.4%	86.8 ± 20.2%	60.8 ± 26.3%
PE/PP	88 ± 3%	95.3 ± 3%	57.3 ± 8.3%	98 ± 1.8%
PET	20.7 ± 8.3%	11.3 ± 7.7%	90 ± 4.1%	36.7 ± 22.9%
PS	100 ± 0%	89.3 ± 23.9%	100 ± 0%	51.3 ± 25.3%
PVC	100 ± 0%	58.7 ± 14.3%	100 ± 0%	57.3 ± 27.6%

	SURFACE WATER WEATHERED MPS		DEEP-SEA WATER WEATHERED MPS	
RANDOM FOREST CLASSIFIER FSM (ILVO)	**PDM**	**PIM**	**PDM**	**PIM**
CCI %	100 ± 0%	99 ± 0.5%	100 ± 0%	99 ± 0.5%
Cohen's κ	1	0.98	1	1
Total number of tested MPs	78.8 ± 36.0% (96.7 ± 5.8% without PET)	70.0 ± 39.2% (88.9 ± 12.8% without PET)	87.8 ± 17.1% (87.6 ± 21 without PET)	80.3 ± 14.8% (84 ± 15.7 without PET)
PE/PP	90 ± 0%	99.3 ± 1.5%	63.3 ± 0%	100 ± 0%
PET	25.3 ± 0.5%	86.7 ± 0%	88.7 ± 0.5%	69.3 ± 1.5%
PS	100 ± 0%	92.7 ± 1.5%	100 ± 0%	83.3 ± 7.8%
PVC	100 ± 0%	74.7 ± 1.8%	99.3 ± 0.4%	68.7 ± 3.8%

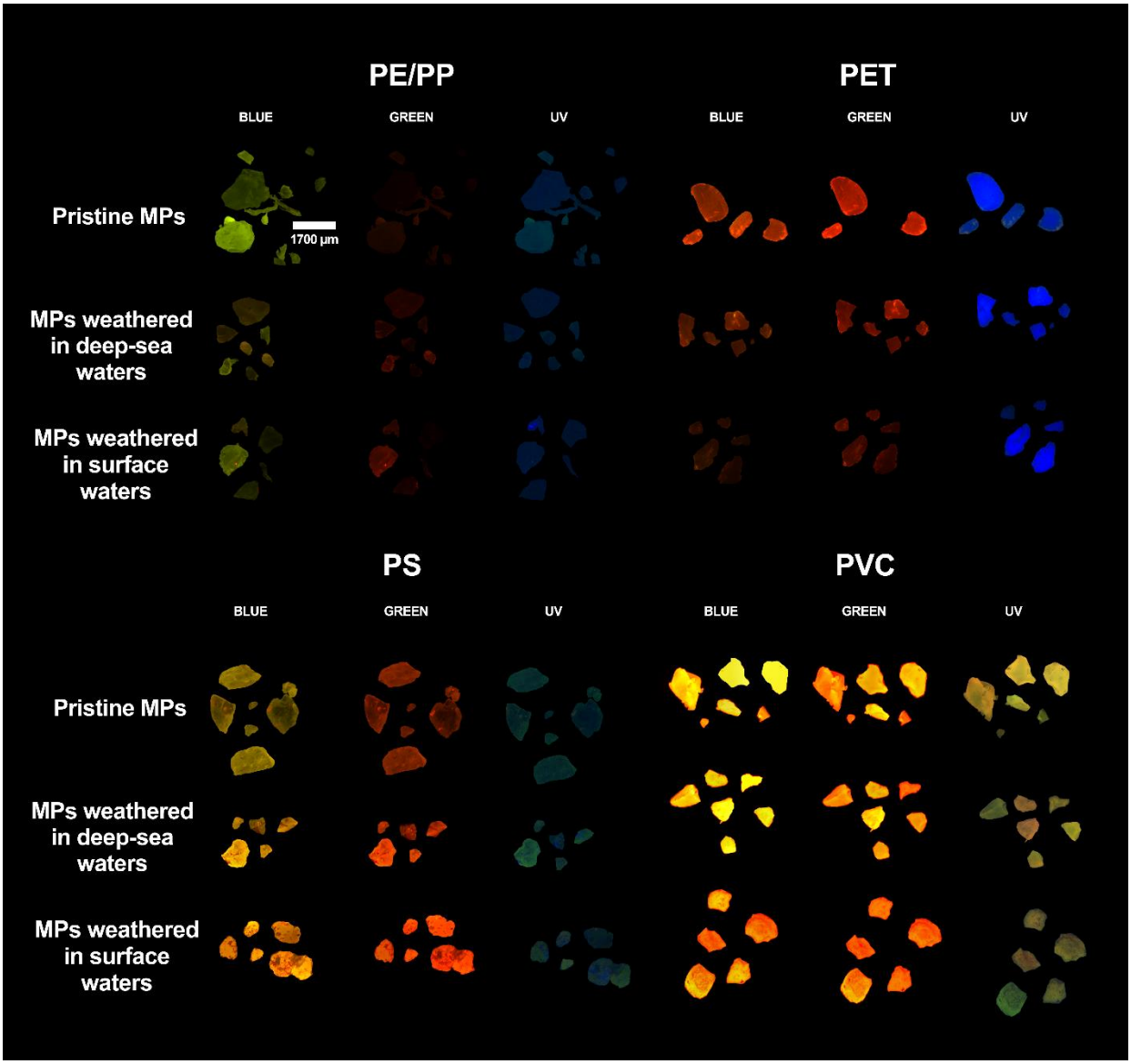

Fig. 4. Stereomicroscopic images of pristine and weathered microplastics. Images of four Nile red-stained, commonly produced microplastic polymers, acquired with a fluorescence stereomicroscope, under a blue, green and UV filter, and used by the models to predict a particle's plastic identity, and to identify its polymer type based on fluorescence colouration and intensity. In this figure, pristine microplastics per polymer type are shown, as well as surface water-weathered microplastics and deep-sea water-weathered microplastics.

3.3 Lower size limit

The VLIZ PDM and PIM both achieved sufficient accuracy (> 70%) for the lowest size class tested across all polymers (Fig. S13, Table S2). This class corresponds to particles with a maximum Feret diameter of 6 to 30 pixels, meaning that predictions were based on the same number of RGB statistics. Under the magnification used, this corresponds to particles < 10 µm. After conversion, the smallest accurately

identified particles were 2 µm (6 pixels) for PET, 4 µm (12 pixels) for both PE/PP and PS, and 4 µm (12 pixels) for PVC. The lower size limit was determined by the smallest particle present on the respective PTFE filters (Table S2).

3.4 Interoperability

To assess the interoperability of the models, the ILVO models were tested on VLIZ datasets 1 and 2, and vice versa. Both models designed for plastic detection demonstrated a robust ability to identify nearly all plastic particles accurately when using the optimised in-lab method, achieving CCI rates of 100 ± 0% (VLIZ models) and 96.9 ± 0.1% (ILVO models). However, the ILVO PDM misclassified certain plastics such as nylon (CCI rate of 98.6 ± 0%) and PUR (80 ± 0.8%), which were unknown to the model (Table 3). Despite the high accuracy in plastic detection, the models showed a significant risk of overprediction. The ILVO models correctly identified only 58.7 ± 0.2% of organic materials photographed in the VLIZ laboratory, while the VLIZ models achieved a mere 0.8 ± 0.4% accuracy for organic materials photographed in the ILVO laboratory.

While the models performed well for polymers like PE/PP (with accuracies ranging from 66.2 ± 4.6% to 100 ± 0%), they were less accurate for other polymers such as PET, PS, and PVC when used with different instrumentation, with CCI rates ranging from 6.8 ± 0.3% to 55.9 ± 3%. These disparities indicate that the models in their current form are unsuitable for generating accurate predictions of particles based on images obtained using different microscope types or magnifications.

Table 3: Interoperability of the RF models. The interoperability of the Plastic Detection Model (PDM) and the Polymer Identification Model (PIM) was tested by analysing MPs in the ILVO datasets 1 and 2, acquired with a fluorescence stereomicroscope (FSM) in the ILVO laboratory, using models based on the VLIZ datasets 1 and 2, respectively, acquired with a fluorescence microscope (FM) in the VLIZ laboratory, and vice versa.

	ILVO MODELS BASED ON FSM – ANALYSED PARTICLES BASED ON FM (VLIZ)		VLIZ MODELS BASED ON FM – ANALYSED PARTICLES BASED ON FSM (ILVO)	
RANDOM FOREST CLASSIFIER	PDM	PIM	PDM	PIM
PE/PP	100 ± 0%	66.2 ± 4.6%	100 ± 0%	100 ± 0%
PET	100 ± 0%	55.9 ± 3%	100 ± 0%	93.2 ± 0.3%
PS	100 ± 0%	78.4 ± 27.4%	100 ± 0%	6.8 ± 0.3%
PVC	100 ± 0%	100 ± 0%	100 ± 0%	18.5 ± 0%
All plastics	96.9 ± 0.1%	73.3 ± 12.6%	100 ± 0%	35.4 ± 48.8%
Organic	58.7 ± 0.2%		0.8 ± 0.4%	

4. Discussion

4.1 Choice of machine learning algorithm

In this research, both DT and RF models demonstrated similarly high accuracies in detecting plastics and identifying the polymer composition of pristine materials. When applied to weathered plastic particles, both models maintained high detection accuracies (SFW: 77.2 ± 38% (DT) vs. 78.8 ± 36% (RF); DSW: 86.8 ± 20% (DT) vs. 87.8 ± 17 (RF)) (Tables 1 and 2). However, for identifying the specific polymers of weathered plastics, only the RF models achieved sufficiently high accuracies (SFW: 63.7 ± 38.4% (DT) vs. 70 ± 39.2% (RF); DSW: 60.8 ± 26.3% (DT) vs. 80.3 ± 14.8 (RF)). Decision tree and RF algorithms represent two prominent and popular ML approaches within MP research (Li et al., 2023; Wu et al., 2023; Yao et al., 2023), each offering advantages and challenges. Decision tree models are more prone to overfitting, which can reduce accuracy on new data. A maximum depth as well as a minimum sample size per node should be specified to prevent the tree from growing endlessly, ensuring the model captures only the most general and crucial aspects of the dataset. Despite these challenges, DTs are valued for their transparency and interpretability. The simplicity of these white box models allows for an easy visualisation, which makes them particularly useful when model clarity is essential.

Random forest models, classified as black box models, are inherently more complex than DTs, which can pose challenges in understanding their internal structure and interpreting the reasoning behind certain predictions. Unlike DTs, RFs do not provide a clear breakdown of weighted scores, but they are generally more robust, effectively handling the instability and overfitting issues that can affect a single DT (Bienefeld et al., 2022). Random forest models can leverage the power of multiple DTs for decision making by creating random subsets of features to build multiple smaller DTs, which are then combined. In qualitative data classification, such as in this study, the predictions of these DTs are aggregated through a majority voting system to produce a final prediction (Svetnik et al., 2003). Although RFs do not require pruning, their performance is sensitive to the number of predictive variables considered. Increasing these variables enhances model strength but also raises intercorrelation, while decreasing them has the opposite effect. Additionally, while increasing the number of trees generally improves predictive accuracy, a threshold exists beyond which there is no significant performance gain anymore. However, with an increasing number of trees to be tested often comes an increased analysis time.

Our study underlines the robustness of the RF algorithm in managing alterations in polymers due to weathering in surface and deep-sea waters. The collective strength of RFs was essential in maintaining a sufficient predictive accuracy despite potential variations in fluorescence colouration and intensity caused by MP weathering. Moreover, the ability of the RF models to mitigate overfitting while enhancing interoperability contributed to their superior performance in capturing potential spectral changes or changes in fluorescence intensity across different polymers. Despite their complexity, the increase in computational costs associated with RF models compared to the DT models was negligible. Therefore, for analyses where both MP quantification and identification are required, RF emerges as the superior algorithm. However, if polymer identification is not a research goal, both DT and RF classifiers allow for a reliable analysis of MPs in a cost- and time-effective manner.

The ability to accurately analyse weathered MPs makes the developed models particularly relevant, as it ensures their applicability to real-world environmental samples. Other studies have also leveraged RF classifiers for MP analysis: Vitali et al., 2024 developed a method for analysing MPs in bottled water using NR staining and an RF-based automated image processing workflow, achieving precise quantification and sizing of MPs down to 10 µm. At the same time, Wang et al., 2024 utilised flow cytometry coupled with ML, including RF algorithms, to effectively differentiate MPs from natural particles in aqueous suspensions. Alternative methods for identifying MP polymer types not based on chemical analysis include

confocal fluorescence microscopy combined with fluorescence life-time imaging microscopy (FLIM), which distinguishes polymers based on emission spectra but has limited validation in real-world samples (Sancataldo et al., 2020). Another approach, using photoluminescence spectroscopy alongside NR staining, differentiates plastics based on their Stokes shift, although the impact of weathering on spectral emission still requires further study (Konde et al., 2020).

The effective application of the new method requires a solid understanding of machine learning techniques, where DTs offer a straightforward and simple interpretation through their transparent inner structure, while the more complex RFs require a specialised knowledge, potentially requiring additional training. Next to this, while the multi-filter approach reduces the number of false positives compared to single-filter methods (Meyers et al., 2022) and enables polymer identification, its increased complexity requires a thorough understanding of the NR staining process, familiarity with the expected fluorescent colouration of reference plastics, and the ability to effectively operate fluorescence microscopes with multiple filters.

4.2 Environmental weathering of microplastics and its consequences for microplastic analysis

The developed models presented in this work leveraged the solvatochromic properties of NR to predict particle identity. The emission spectrum of NR shifts based on the polarity of its environment, which allows for distinguishing MPs into "polar" and "hydrophobic" categories according to their polymer characteristics (Maes et al., 2017). As polymer polarity increases, the maximum emission wavelengths shift towards longer wavelengths, facilitating further classification into specific polymer types through quantification of their fluorescent colouration (Meyers et al., 2022). Notably, the fluorescent colouration of SFW PET particles following NR staining substantially differed from that of pristine PET particles, a change not observed in DSW PET particles (Fig. 4). This suggests susceptibility of this polymer to weathering processes that are more dominant in sea-surface waters, such as UV radiation and microorganism settlement. To improve the accuracy of predictions for polymers like PET, it is recommended to include RGB data from weathered particles in the training datasets. This can be achieved through artificial weathering processes or semi-controlled environmental weathering, as implemented in this study. Incorporating such data would likely enhance the overall predictive accuracy of the models. Alternatively, RGB datasets could be constructed using naturally weathered MPs, although this approach may be more labour- and time-intensive.

Plastic waste typically decomposes slowly but weathers and breaks down into MPs when exposed to UV radiation, mechanical abrasion, temperature changes, and biodegradation. These weathering processes rapidly alter the physical and chemical properties of MPs, affecting their environmental behaviour, including increased leaching of additives, changes in molecular weight and surface roughness, and enhanced pollutant absorption due to biofilm formation (Liu et al., 2019; Duan et al., 2021). The absence of a pretreatment step, which generally applies for water samples low in organic content (Gago et al., 2019), may have allowed biofilm residues to remain on the MPs, potentially affecting NR staining and fluorescence analysis. A recent validation study from our laboratory that employed digestion methods (Meyers et al., 2024) demonstrated higher accuracy in identifying weathered MPs, with 98.25 ± 3.04% of DSW MPs and 100% of SFW MPs correctly identified by the PDM. The slightly lower accuracy observed in the current study (78.8 ± 36% for SFW MPs and 87.8 ± 17% for DSW MPs) may be attributed to the presence and costaining of biofilms on the untreated MPs (Macedo et al., 2005). The polymer identification accuracy for weathered plastics was similar in both studies.

Environmental ageing processes pose challenges for MP analysis methods, which are often designed and tested using pristine MPs. As became apparent from the obtained results, weathering-induced changes in chemical and physical properties can affect the fluorescent colouration of NR-stained MPs, hindering accurate model classification. Standard Raman and IR spectra of MPs are also affected by aging, leading to shifts that complicate matching with commercial libraries of pristine materials (Fig. S8-S12) (Dong et al., 2020). Developing reference libraries based on naturally weathered MPs could address this issue, but it may increase total analysis time and labour costs. However, adding weathered MP spectra to commercial libraries of pristine MPs has also been shown to improve spectral matching accuracy for environmental samples (De Frond et al., 2021). The ATR spectra generated during this study have been made publicly available (Meyers et al., 2024c). Weathering-induced polymer alterations and potential changes in associated additives may also complicate identification and quantification based on mass spectrometry, another frequently employed analysis (Primpke et al., 2020a). In addition to this, weathering processes may interfere with the step preceding the analysis, where samples are extracted from sample matrices. Environmental degradation has been shown to alter the densities of certain polymers (Kowalski et al., 2016), potentially making it more difficult to efficiently isolate all MPs present in sediment samples.

4.3 Weathered reference plastics

Researchers are increasingly recognising the importance of using reference materials that mimic the properties of weathered MPs when developing and testing new methods, next to the incorporation of a variety of MP polymers, sizes and shapes. This study employed a unique approach by weathering a mix of MPs at sea under semi-controlled surface water and deep-sea water conditions for 12 months, offering a compromise between controlled laboratory simulations and the weathering of MPs under untraceable natural conditions. By adopting this approach, we address inherent challenges associated with both methodologies: unlike conventional laboratory experiments, the weathering process took place under authentic natural conditions. Consequently, the MPs within the containers were exposed to the combined effects of diverse degradation processes and various influencing factors. Periodic cleaning of the surface water containers ensured unobstructed water flow, facilitating natural biodegradation processes. However, the degree of UV weathering in the surface weathering experiment might have been influenced by the experimental setup, as sunlight only partially passed through the container pores. Similarly, the impact of sea wave force may have been partially mitigated by the container. Nevertheless, this setup was imperative for the controlled natural degradation of MPs within the confines of the container. Despite being potentially less labour- and time-intensive compared to the collection of weathered MPs/the collection and cryomilling of weathered macroplastics, the duration of degradation was set to a period of one year in order to be meaningful. As a last point, despite introducing heterogeneity in shape, the process of cryomilling to produce the used MP fragments did not mimic mechanical weathering to the full extent, as various processes such as stretching, tearing, and crushing also contribute to plastic fragmentation in a marine context. Consequently, crucial MP characteristics for risk assessments, such as particle size, do not fully align with the naturally occurring composition. However, in contrast to environmentally sourced MPs with unknown origins and history, the precise deployment location and bathymetric conditions were known and controlled for, along with the duration of weathering. Meteorological conditions, currents, weather patterns, and UV radiation can be retrospectively traced, and can provide a comprehensive understanding if required. Additionally, the study employed a MP composition of the most prevalently produced and encountered plastics, which enhances the global applicability of the results. Lastly, the MPs in this study underwent a weathering duration of 12 months, surpassing the temporal scope of many prior studies (e.g. Naik et al., 2020). Nonetheless, it is acknowledged that certain MPs require multiple years to exhibit substantial weathering effects (Chamas et al., 2020). Alternatively, environmentally relevant weathered MP samples can be produced by cryomilling plastic macrolitter collected from beaches (Kühn et al., 2018).

Future prospects of the approach applied in this work include deployments of weathering containers over prolonged durations to accurately reflect long-term degradation processes, while the generation of MPs through mechanical abrasion processes representative of the marine environment should be pursued. Next to this, refinements in experimental setup are required to ensure unhindered exposure of MPs to sunlight and mechanical forces.

4.3 Lower size limit

The RF models in this study showed an accuracy > 90% for particles with Feret diameters between 12 and 30 pixels,corresponding to MPs < 10 µm at the microscope magnification used. The ability to identify MPs of ecotoxicologically relevant sizes (Beiras et al., 2020) in a cost- and time-effective way enhances the ecological relevance of the method and fills a critical gap. Other frequently used MP analysis methods show similar lower size limits, e.g. 1 µm for µ-Raman and 10 - 20 µm for µ-FTIR (Cabernard et al., 2018; Mintenig et al., 2019; Primpke et al., 2020a). Although no MP size limitation exists for GC-MS-based techniques, a significant drawback is their inability to quantify or characterise MPs physically, information that is essential for risk evaluations (Schwarzer et al., 2022, Qiao et al., 2019). In prior research, NR co-staining of organic material like residual fat posed challenges for NR-based MP analysis (Prata et al., 2021). Efficient matrix removal is crucial but often not feasible, risking inaccuracies in MP detection/quantification (Shruti et al., 2022). In this study, however, the use of multiple filters (UV, blue, green) and the inclusion of fluorescence data unique to organic materials and distinct from plastic into the RF models helped to differentiate between these materials. Additionally, the risk of persistent false positives due to similar fluorescence could be reduced using customised RGB datasets (cfr. '4.4 Interoperability').

Other methods have also succeeded in detecting smaller MPs using a NR-based approach. For example, Ko et al., 2024 introduced a system combining fluorescence labelling with a microfluidic device and particle tracking software, enabling automated size measurement and real-time discrimination of MPs sized 100–1000 nm, such as PS and PVC, in small water samples. Similarly, Bianco et al., 2022 developed a method combining NR staining and flow cytometry and was able to quantify plastic particles in the 0.6–15 µm size range.

721

722 4.4 Interoperability

723 Ensuring consistent method performance across different laboratories is crucial in scientific research and
724 environmental monitoring. When comparing the performance of models built and tested with distinct
725 microscopes, both demonstrated high accuracies for pristine materials. However, during the
726 interoperability assessment, the accuracy of the RF algorithm decreased when models were built and
727 tested using images acquired with different microscope types. Implementing a preprocessing pipeline as
728 a normalisation step to address differences in image acquisition parameters, or leveraging transfer
729 learning, could help tackle this issue. Another option is the development of new datasets. While this
730 outcome presents a challenge, it is important to note that the foundation of the method lies in training
731 datasets which can be easily and rapidly constructed for a specific laboratory (Meyers et al., 2022). For
732 instance, using a fluorescence stereomicroscope (FSM), over 100 reference particles sized < 500 µm can
733 be filtered onto a single PTFE filter and captured in a single image series (blue, green, and UV filters),
734 enabling the construction of an RGB dataset within a day following staining. To enhance predictive
735 robustness, it is however recommended to include RGB data from MPs stained with NR at different points
736 in time. Building a training dataset, constructing a model, and testing its accuracy can be completed in
737 two days. This inherent flexibility of the method allows for its swift adaptation and optimisation, in this
738 way ensuring the possibility to fine-tune the method to specific laboratory conditions and set
739 requirements. In this way, researchers can account for unique variables in their own research that could
740 potentially affect model performance, such as 1) the specific MP polymer composition being targeted, 2)
741 the matrix type from which these MPs are extracted and which may interact with the MPs' NR
742 fluorescence, 3) the specific types of organic material present in that matrix which could interfere with
743 MP detections (e.g. chitin in seawater samples or lipid residues in gastrointestinal tracts (GITs) of fish), 4)
744 the microscope model and magnification used to perform the analyses, and so on. Consequently, the
745 lower accuracy obtained when testing the interoperability of the models does not impede their
746 implementation elsewhere. Instead, it emphasises the adaptability of the developed method. Giving
747 laboratories the ability to efficiently create customised datasets allows them to address specific
748 challenges encountered, thereby strengthening the robustness of the method and its successful
749 deployment in diverse environments.

750

751 Additionally, this cost-effective approach is particularly beneficial for laboratories that lack the expensive
752 equipment often associated with MP analysis (Primpke et al., 2020a). In this way, the approach enables a

broader range of laboratories to engage in MPs research, facilitating the advancement of knowledge on plastic pollution across diverse marine environments worldwide.

5. Conclusion

Both DT and RF models demonstrated high accuracy in detecting pristine and weathered MPs. Despite their complexity, RF models are preferred for polymer identification due to their superior performance and minimal increase in computational time. Although the models generally had a high predictive reliability, incorporating RGB data from weathered particles could further enhance accuracy for specific polymers like PET. The models also proved effective in detecting and identifying MPs smaller than 10 µm, underlining their potential in analysing ecotoxicologically relevant MPs in marine environments. Although interlaboratory assessments revealed challenges related to microscope type variations, the adaptability of the RF models allows customisation to specific conditions, ensuring robustness and successful application in diverse settings.

The relevance and novelty of the method are underscored by its ability to accurately analyse MPs weathered under various marine conditions, making it highly applicable to real-world environmental samples. Additionally, its capability to detect ecotoxicologically relevant MP sizes in a cost- and time-effective manner addresses a critical gap in MP research. Moreover, by providing a cost- and time-effective alternative to traditional methods, the ML-based method enables a wide range of laboratories to engage in MP research.

Acknowledgments

The authors thank the captain and crew of the R/V Antedon II (Flotte Océanographique Française), as well as Deny Malengros, Laure Papillon and Mélanie Ourgaud for their assistance in the deployment and retrieval of the deep-sea samples. We also thank Mattias Bossaer from VLIZ for assisting in the acquisition of ATR spectra of both pristine and weathered microplastics. Lastly, we thank the partners of the JPI Oceans Andromeda project who supported this work, as well as BELSPO, RBINS OD Nature, the Pluxin project, the French Agence Nationale de Recherche (ANR-19-383 JOCE-0002-01) and the Norwegian Research Council (311313/E40) for funding or for financing ship time.

Appendix A. Supplementary data

Supplementary data to this article can be found online at:

Ethical Approval

Not applicable

Consent to Participate

Not applicable

Consent to Publish

Not applicable

Data availability

The RGB colour datasets of all models are freely available: https://doi.org/10.14284/665. Other data will be made available on reasonable request.

Authors Contributions

Nelle Meyers: Conceptualisation, Data curation, Formal analysis, Investigation, Methodology, Project administration, Software, Validation, Visualisation, Writing – original draft, Writing – review & editing. **Bavo De Witte**: Conceptualisation, Methodology, Project administration, Supervision, Funding acquisition, Writing – review & editing. **Natascha Schmidt**: Conceiving, designing, and performing of weathering experiments, Writing – review & editing. **Dorte Herzke**: Conceiving, designing, and performing of weathering experiments, Funding acquisition, Writing – review & editing. **Jean-Luc Fuda**: Conceiving,

designing, and performing of weathering experiments, Writing – review & editing. **David Vanavermaete**: Methodology, Software, Writing – review & editing. **Colin Janssen**: Supervision, Funding acquisition, Writing – review & editing. **Gert Everaert**: Conceptualisation, Methodology, Project administration, Supervision, Funding acquisition, Writing – review & editing.

Funding

This work was supported by the Andromeda project (JPI Oceans). We thank BELSPO [contract no B2/20E/P1/Andromeda], the Pluxin project, the French Agence Nationale de Recherche (ANR-19-383 JOCE-0002-01) and the Norwegian Research Council (311313/E40) for funding.

Competing interests

The authors declare that they have no known competing financial interests or personal relationships that could have appeared to influence the work reported in this paper.

References

Abràmoff, M.D., Magalhães, P.J. and Ram, S.J., 2004. Image processing with ImageJ. Biophotonics international, 11(7), pp.36-42.

Alimi, O.S., Claveau-Mallet, D., Kurusu, R.S., Lapointe, M., Bayen, S. and Tufenkji, N., 2022. Weathering pathways and protocols for environmentally relevant microplastics and nanoplastics: What are we missing?. Journal of Hazardous Materials, 423, p.126955.

Arp, H.P.H., Kühnel, D., Rummel, C., MacLeod, M., Potthoff, A., Reichelt, S., Rojo-Nieto, E., Schmitt-Jansen, M., Sonnenberg, J., Toorman, E. and Jahnke, A., 2021. Weathering plastics as a planetary boundary threat: exposure, fate, and hazards. Environmental science & technology, 55(11), pp.7246-7255.

Arthur, C., Baker, J.E. and Bamford, H.A., 2009. Proceedings of the International Research Workshop on the Occurrence, Effects, and Fate of Microplastic Marine Debris, September 9-11, 2008, University of Washington Tacoma, Tacoma, WA, USA.

Beiras, R. and Schönemann, A.M., 2020. Currently monitored microplastics pose negligible ecological risk to the global ocean. Scientific reports, 10(1), p.22281.

Bergmann, M., Mützel, S., Primpke, S., Tekman, M.B., Trachsel, J. and Gerdts, G., 2019. White and wonderful? Microplastics prevail in snow from the Alps to the Arctic. Science advances, 5(8), p.eaax1157.

Bhagat, K., Barrios, A.C., Rajwade, K., Kumar, A., Oswald, J., Apul, O. and Perreault, F., 2022. Aging of microplastics increases their adsorption affinity towards organic contaminants. Chemosphere, 298, p.134238.

Bianco, A., Carena, L., Peitsaro, N., Sordello, F., Vione, D. and Passananti, M., 2023. Rapid detection of nanoplastics and small microplastics by Nile-Red staining and flow cytometry. Environmental Chemistry Letters, 21(2), pp.647-653.

Bienefeld, C., Kirchner, E., Vogt, A. and Kacmar, M., 2022. On the importance of temporal information for remaining useful life prediction of rolling bearings using a random forest regressor. Lubricants, 10(4), p.67.

Breiman, L., Friedman, J.H., Olshen, R.A., Stone,C.J. Classification and Regression Trees, Chapman & Hall, 1993.

Breiman, L., 1996. Bagging predictors. Machine learning, 24, pp.123-140.

Breiman, L., 2001. Random forests. Machine learning, 45, pp.5-32.

Cabernard, L., Roscher, L., Lorenz, C., Gerdts, G. and Primpke, S., 2018. Comparison of Raman and Fourier transform infrared spectroscopy for the quantification of microplastics in the aquatic environment. Environmental science & technology, 52(22), pp.13279-13288.

Catarino, A.I., Kramm, J., Voelker, C., Henry, T.B. and Everaert, G., 2021. Risk posed by microplastics: Scientific evidence and public perception. Current Opinion in Green and Sustainable Chemistry, 29, p.100467.

Chamas, A., Moon, H., Zheng, J., Qiu, Y., Tabassum, T., Jang, J.H., Abu-Omar, M., Scott, S.L. and Suh, S., 2020. Degradation rates of plastics in the environment. ACS Sustainable Chemistry & Engineering, 8(9), pp.3494-3511.

Cowger, W., Gray, A., Christiansen, S.H., DeFrond, H., Deshpande, A.D., Hemabessiere, L., Lee, E., Mill, L., Munno, K., Ossmann, B.E. and Pittroff, M., 2020. Critical review of processing and classification techniques for images and spectra in microplastic research. Applied Spectroscopy, 74(9), pp.989-1010.

Daniya, T., Geetha, M. and Kumar, K.S., 2020. Classification and regression trees with gini index. Advances in Mathematics: Scientific Journal, 9(10), pp.8237-8247.

Dong, M., Zhang, Q., Xing, X., Chen, W., She, Z. and Luo, Z., 2020. Raman spectra and surface changes of microplastics weathered under natural environments. Science of The Total Environment, 739, p.139990.

Duan, J., Bolan, N., Li, Y., Ding, S., Atugoda, T., Vithanage, M., Sarkar, B., Tsang, D.C. and Kirkham, M.B., 2021. Weathering of microplastics and interaction with other coexisting constituents in terrestrial and aquatic environments. Water Research, 196, p.117011.

Dunford, R., Su, Q. and Tamang, E., 2014. The pareto principle.

Fauvelle, V., Garel, M., Tamburini, C., Nerini, D., Castro-Jiménez, J., Schmidt, N., Paluselli, A., Fahs, A., Papillon, L., Booth, A.M. and Sempéré, R., 2021. Organic additive release from plastic to seawater is lower under deep-sea conditions. Nature Communications, 12(1), p.4426.

Fotopoulou, K.N. and Karapanagioti, H.K., 2019. Degradation of various plastics in the environment. Hazardous chemicals associated with plastics in the marine environment, pp.71-92.

Gago, J., Filgueiras, A., Pedrotti, M.L., Caetano, M. and Frias, J., 2019. Standardised protocol for monitoring microplastics in seawater. Deliverable 4.1.
.

Guo, P., Wang, Y., Moghaddamfard, P., Meng, W., Wu, S. and Bao, Y., 2024. Artificial intelligence-empowered collection and characterization of microplastics: A review. Journal of Hazardous Materials, p.134405.

Harris-Birtill, D. and Harris-Birtill, R., 2021. Understanding computation time: a critical discussion of time as a computational performance metric. In Time in Variance (pp. 220-248). Brill.

Hartmann, N.B., Huffer, T., Thompson, R.C., Hassellov, M., Verschoor, A., Daugaard, A.E., Rist, S., Karlsson, T., Brennholt, N., Cole, M. and Herrling, M.P., 2019. Are we speaking the same language? Recommendations for a definition and categorization framework for plastic debris.

Kiki, C., Qiu, Y., Wang, Q., Ifon, B.E., Qin, D., Chabi, K., Yu, C.P., Zhu, Y.G. and Sun, Q., 2022. Induced aging, structural change, and adsorption behavior modifications of microplastics by microalgae. Environment International, 166, p.107382.

Kinigopoulou, V., Pashalidis, I., Kalderis, D. and Anastopoulos, I., 2022. Microplastics as carriers of inorganic and organic contaminants in the environment: A review of recent progress. Journal of Molecular Liquids, 350, p.118580.

Ko, K. and Chung, H., 2024. Fluorescence microfluidic system for real-time monitoring of PS and PVC sub-micron microplastics under flowing conditions. Science of The Total Environment, 950, p.175016.

Kolandhasamy, P., Su, L., Li, J., Qu, X., Jabeen, K. and Shi, H., 2018. Adherence of microplastics to soft tissue of mussels: a novel way to uptake microplastics beyond ingestion. Science of the total environment, 610, pp.635-640.

Konde, S., Ornik, J., Prume, J.A., Taiber, J. and Koch, M., 2020. Exploring the potential of photoluminescence spectroscopy in combination with Nile Red staining for microplastic detection. Marine Pollution Bulletin, 159, p.111475.

Kowalski, N., Reichardt, A.M. and Waniek, J.J., 2016. Sinking rates of microplastics and potential implications of their alteration by physical, biological, and chemical factors. Marine pollution bulletin, 109(1), pp.310-319.

Kühn, S., Van Oyen, A., Booth, A.M., Meijboom, A. and Van Franeker, J.A., 2018. Marine microplastic: Preparation of relevant test materials for laboratory assessment of ecosystem impacts. Chemosphere, 213, pp.103-113.

Li, W., Li, X., Tong, J., Xiong, W., Zhu, Z., Gao, X., Li, S., Jia, M., Yang, Z. and Liang, J., 2023. Effects of environmental and anthropogenic factors on the distribution and abundance of microplastics in freshwater ecosystems. Science of The Total Environment, 856, p.159030.

Liaw, A. and Wiener, M., 2002. Classification and regression by randomForest. R news, 2(3), pp.18-22.

Lin, J.Y., Liu, H.T. and Zhang, J., 2022. Recent advances in the application of machine learning methods to improve identification of the microplastics in environment. Chemosphere, p.136092.

Liu, P., Qian, L., Wang, H., Zhan, X., Lu, K., Gu, C. and Gao, S., 2019. New insights into the aging behavior of microplastics accelerated by advanced oxidation processes. Environmental science & technology, 53(7), pp.3579-3588.

Liu, P., Zhan, X., Wu, X., Li, J., Wang, H. and Gao, S., 2020. Effect of weathering on environmental behavior of microplastics: Properties, sorption and potential risks. Chemosphere, 242, p.125193.

Liu, R., Wang, Y., Yang, Y., Shen, L., Zhang, B., Dong, Z., Gao, C. and Xing, B., 2023. New insights into adsorption mechanism of pristine and weathered polyamide microplastics towards hydrophilic organic compounds. Environmental Pollution, 317, p.120818.

Maes, T., Jessop, R., Wellner, N., Haupt, K. and Mayes, A.G., 2017. A rapid-screening approach to detect and quantify microplastics based on fluorescent tagging with Nile Red. Scientific reports, 7(1), p.44501.

Mattsson, K., Jocic, S., Doverbratt, I. and Hansson, L.A., 2018. Nanoplastics in the aquatic environment. Microplastic contamination in aquatic environments, pp.379-399.

Maxwell, A.E., Warner, T.A. and Fang, F., 2018. Implementation of machine-learning classification in remote sensing: An applied review. International journal of remote sensing, 39(9), pp.2784-2817.

McHugh, M.L., 2012. Interrater reliability: the kappa statistic. Biochemia medica, 22(3), pp.276-282.

Meyers, N., Catarino, A.I., Declercq, A.M., Brenan, A., Devriese, L., Vandegehuchte, M., De Witte, B., Janssen, C. and Everaert, G., 2022. Microplastic detection and identification by Nile red staining: Towards a semi-automated, cost-and time-effective technique. Science of the Total Environment, 823, p.153441.

Meyers, N.; De Witte, B.; Catarino, A. I.; & Everaert, G. 2024a. Standardised operating protocol for automated microplastic analysis using machine learning models. JPI Oceans Andromeda Project.

Meyers, N.; De Witte, B.; Janssen, C.; Everaert, G.; Flanders Marine Institute (VLIZ); Flanders Research Institute for Agriculture, Fisheries and Food (ILVO); Ghent University Laboratory for Environmental Toxicology (GhEnToxLab): Belgium; 2024b: RGB datasets for machine learning-based microplastic analysis - update. Marine Data Archive. https://doi.org/10.14284/665

Meyers, N.; De Witte, B.; Schmidt, N.; Herzke, D.; Fuda, J.; Vanavermaete, D; Bossaer, M.; Janssen, C.; Everaert, G. 2024c. Infrared spectra of plastic polymers weathered in the marine environment under semi-controlled conditions. https://doi.org/10.14284/664

Meyers, N., Everaert, G., Hostens, K., Schmidt, N., Herzke, D., Fuda, J.L., Janssen, C.R. and De Witte, B., 2024. Towards reliable data: Validation of a machine learning-based approach for microplastics analysis in marine organisms using Nile red staining. *Marine Pollution Bulletin*, *207*, p.116804.

Mintenig, S.M., Löder, M.G., Primpke, S. and Gerdts, G., 2019. Low numbers of microplastics detected in drinking water from ground water sources. Science of the total environment, 648, pp.631-635.

Naik, R.A., Rowles III, L.S., Hossain, A.I., Yen, M., Aldossary, R.M., Apul, O.G., Conkle, J. and Saleh, N.B., 2020. Microplastic particle versus fiber generation during photo-transformation in simulated seawater. Science of The Total Environment, 736, p.139690.

Paradinas, L.M., James, N.A., Quinn, B., Dale, A. and Narayanaswamy, B.E., 2021. A new collection tool-kit to sample microplastics from the marine environment (sediment, seawater, and biota) using citizen science. Frontiers in Marine Science, 8, p.657709.

Peeken, I., Primpke, S., Beyer, B., Gütermann, J., Katlein, C., Krumpen, T., Bergmann, M., Hehemann, L. and Gerdts, G., 2018. Arctic sea ice is an important temporal sink and means of transport for microplastic. Nature communications, 9(1), p.1505.

Peng, X., Chen, M., Chen, S., Dasgupta, S., Xu, H., Ta, K., Du, M., Li, J., Guo, Z. and Bai, S., 2018. Microplastics contaminate the deepest part of the world's ocean. Geochemical Perspectives Letters, 9(1), pp.1-5.

Prata, J.C., Sequeira, I.F., Monteiro, S.S., Silva, A.L.P., da Costa, J.P., Dias-Pereira, P., Fernandes, A.J.S., da Costa, F.M., Duarte, A.C., Rocha-Santos, T., 2021. Preparation of biological samples for microplastic identification by Nile Red. Sci. Total Environ. 783, 147065.

Primpke, S., Christiansen, S.H., Cowger, W., De Frond, H., Deshpande, A., Fischer, M., Holland, E.B., Meyns, M., O'Donnell, B.A., Ossmann, B.E. and Pittroff, M., 2020a. Critical assessment of analytical methods for the harmonized and cost-efficient analysis of microplastics. Applied Spectroscopy, 74(9), pp.1012-1047.

Primpke, S., Cross, R.K., Mintenig, S.M., Simon, M., Vianello, A., Gerdts, G. and Vollertsen, J., 2020b. Toward the systematic identification of microplastics in the environment: evaluation of a new independent software tool (siMPle) for spectroscopic analysis. 2020b. Applied Spectroscopy, 74(9), pp.1127-1138.

Qiao, R., Deng, Y., Zhang, S., Wolosker, M. B., Zhu, Q., Ren, H., & Zhang, Y. (2019). Accumulation of different shapes of microplastics initiates intestinal injury and gut microbiota dysbiosis in the gut of zebrafish. Chemosphere, 236, 124334.

Ross, P.S., Chastain, S., Vassilenko, E., Etemadifar, A., Zimmermann, S., Quesnel, S.A., Eert, J., Solomon, E., Patankar, S., Posacka, A.M. and Williams, B., 2021. Pervasive distribution of polyester fibres in the Arctic Ocean is driven by Atlantic inputs. Nature communications, 12(1), p.106.

Sancataldo, G., Avellone, G. and Vetri, V., 2020. Nile Red lifetime reveals microplastic identity. Environmental Science: Processes & Impacts, 22(11), pp.2266-2275.

Serdar, C.C., Cihan, M., Yücel, D. and Serdar, M.A., 2021. Sample size, power and effect size revisited: simplified and practical approaches in pre-clinical, clinical and laboratory studies. Biochemia medica, 31(1), pp.27-53.

Shah, A.A., Hasan, F., Hameed, A. and Ahmed, S., 2008. Biological degradation of plastics: a comprehensive review. Biotechnology advances, 26(3), pp.246-265.

Shruti, V.C., Pérez-Guevara, F., Roy, P.D., Kutralam-Muniasamy, G., 2022. Analyzing microplastics with Nile red: emerging trends, challenges, and prospects. J. Hazard. Mater. 423, 127171.

Svetnik, V., Liaw, A., Tong, C., Culberson, J.C., Sheridan, R.P. and Feuston, B.P., 2003. Random forest: a classification and regression tool for compound classification and QSAR modeling. Journal of chemical information and computer sciences, 43(6), pp.1947-1958.

Schwarzer, M., Brehm, J., Vollmer, M., Jasinski, J., Xu, C., Zainuddin, S., Fröhlich, T., Schott, M., Greiner, A., Scheibel, T. & Laforsch, C. (2022). Shape, size, and polymer dependent effects of microplastics on Daphnia magna. Journal of Hazardous Materials, 426, 128136.

Therneau, T., Atkinson, B., Ripley, B. and Ripley, M.B., 2015. Package 'rpart'. Available online: cran. ma. ic. ac. uk/web/packages/rpart/rpart. pdf (accessed on 20 April 2016).

Van Cauwenberghe, L., Vanreusel, A., Mees, J. and Janssen, C.R., 2013. Microplastic pollution in deep-sea sediments. Environmental pollution, 182, pp.495-499.

Vitali, C., Peters, R.J., Janssen, H.G., Undas, A.K., Munniks, S., Ruggeri, F.S. and Nielen, M.W., 2024. Quantitative image analysis of microplastics in bottled water using artificial intelligence. Talanta, 266, p.124965.

Yan, X., Cao, Z., Murphy, A. and Qiao, Y., 2022. An ensemble machine learning method for microplastics identification with FTIR spectrum. Journal of Environmental Chemical Engineering, 10(4), p.108130.

Wagner, S. and Reemtsma, T., 2019. Things we know and don't know about nanoplastic in the environment. Nature nanotechnology, 14(4), pp.300-301.

Waldman, W.R. and Rillig, M.C., 2020. Microplastic research should embrace the complexity of secondary particles.

Wang, L., Zhang, J., Huang, W. and He, Y., 2023. Laboratory simulated aging methods, mechanisms and characteristic changes of microplastics: A review. Chemosphere, p.137744.

Wang, X., Li, Y., Kroll, A. and Mitrano, D.M., 2024. Differentiating Microplastics from Natural Particles in Aqueous Suspensions Using Flow Cytometry with Machine Learning. Environmental Science & Technology.

Wayman, C. and Niemann, H., 2021. The fate of plastic in the ocean environment–a minireview. Environmental Science: Processes & Impacts, 23(2), pp.198-212.

Weis, J.S. and Palmquist, K.H., 2021. Reality check: experimental studies on microplastics lack realism. Applied Sciences, 11(18), p.8529.

Witten, I.H. and Frank, E., 2002. Data mining: practical machine learning tools and techniques with Java implementations. Acm Sigmod Record, 31(1), pp.76-77.

World Health Organization, 2022. Dietary and inhalation exposure to nano-and microplastic particles and potential implications for human health.

Wu, P., Wang, B., Lu, Y., Cao, G., Xie, P., Wang, W., Chen, D., Huang, G., Jin, H., Yang, Z. and Cai, Z., 2023. Machine Learning-Assisted Insights into Sources and Fate of Microplastics in Wastewater Treatment Plants. ACS ES&T Water.

Yao, J., Li, H. and Yang, H.Y., 2023. Predicting adsorption capacity of pharmaceuticals and personal care products on long-term aged microplastics using machine learning. Journal of Hazardous Materials, 458, p.131963.